

Fermilab

Accelerator Physics Center

Exploring Parameter Space for Radiation Effects in SC Magnets

Nikolai Mokhov

Fermilab

With contributions from A. Konobeyev,
V. Pronskikh and S. Striganov



WAMSDO 2011 - Workshop on
Accelerator Magnet, Superconductor,
Design and Optimization - Monday 14

November 2011

OUTLINE

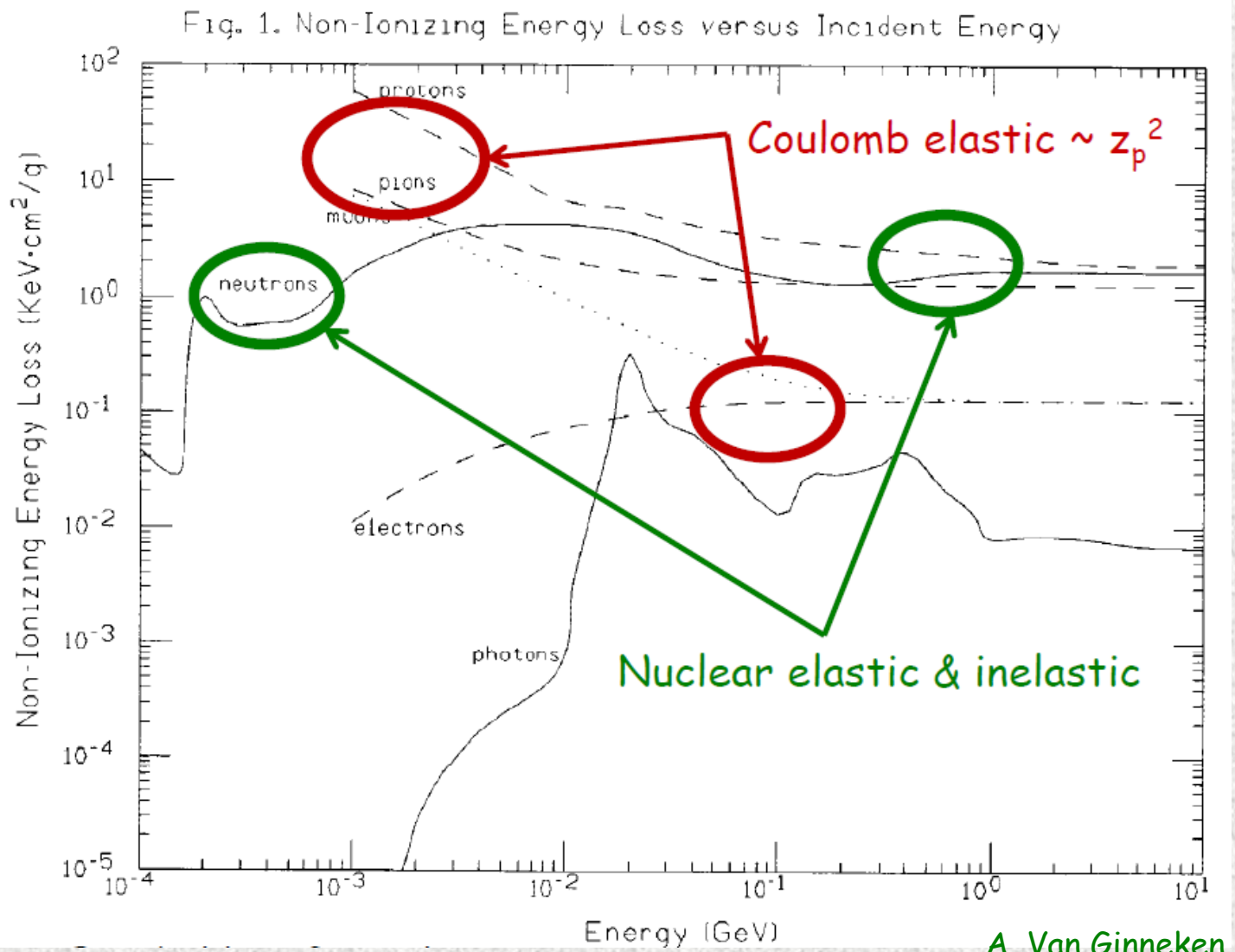
1. DPA and its Modeling
2. DPA Benchmarking
3. LHC Inner Triplet: Full & Toy Models
4. Dose and DPA Composition in SC Coils

Introduction

Deterioration of critical properties of crystalline materials under irradiation is usually analyzed as a function of displacements per atom (DPA). The latter is a strong function of projectile type, energy and charge as well as material properties including its temperature. Radiation effects at high energies are amplified by increased helium gas production.

Some of these dependencies are analyzed here for superconducting coils of LHC inner triplet quadrupoles.

DPA/NIEL vs Particle Type & Energy in Si

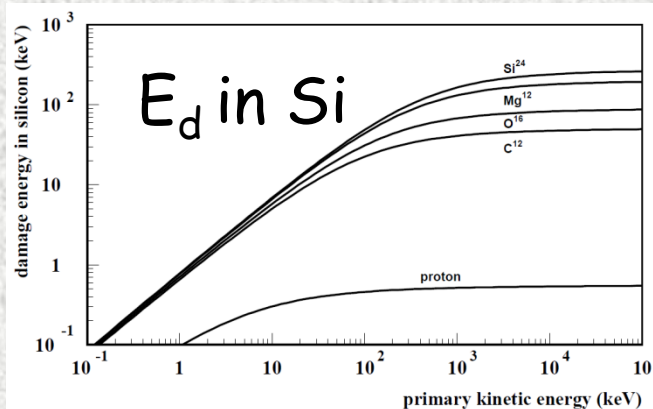


DPA Model in MARS15 (in one slide)

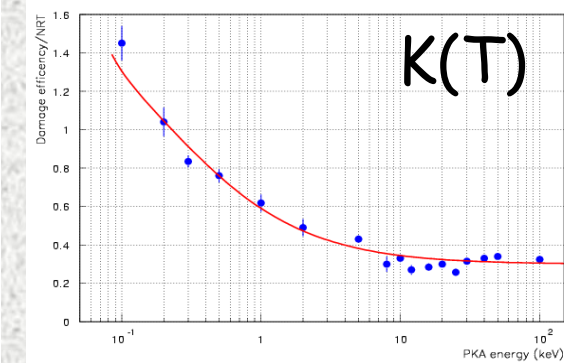
Norgett, Robinson, Torrens (NRT) model for atomic displacements per target atom (DPA) caused by primary knock-on atoms (PKA), created in elastic particle-nucleus collisions, with sequent cascades of atomic displacements (via modified Kinchin-Pease damage function $v(T)$), displacement energy T_d (irregular function of atomic number) and displacement efficiency $K(T)$.

$$\sigma_d(E) = \int_{T_d}^{T_{\max}} \frac{d\sigma(E, T)}{dT} v(T) dT$$

$$v(T) = \begin{cases} 0 & T < T_d \\ 1 & T_d \leq T < 2.5T_d \\ k(T)E_d / 2T_d & 2.5T_d \leq T \end{cases}$$



M. Robinson (1970)

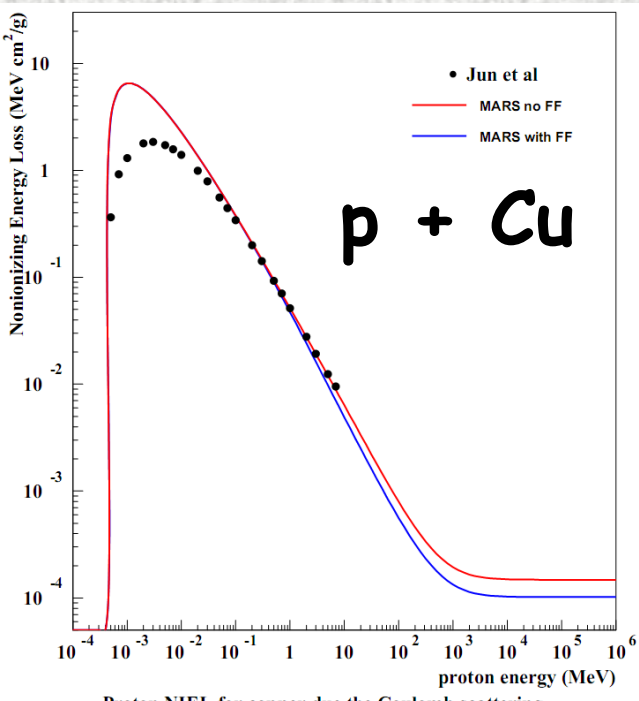
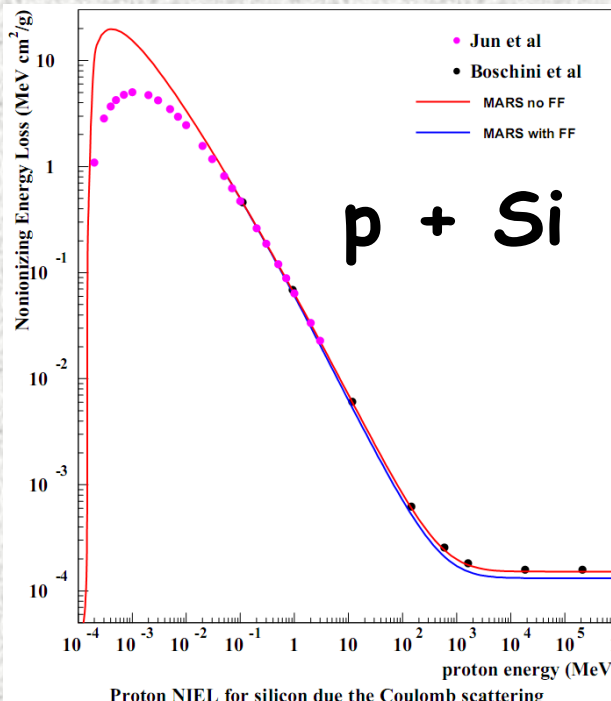
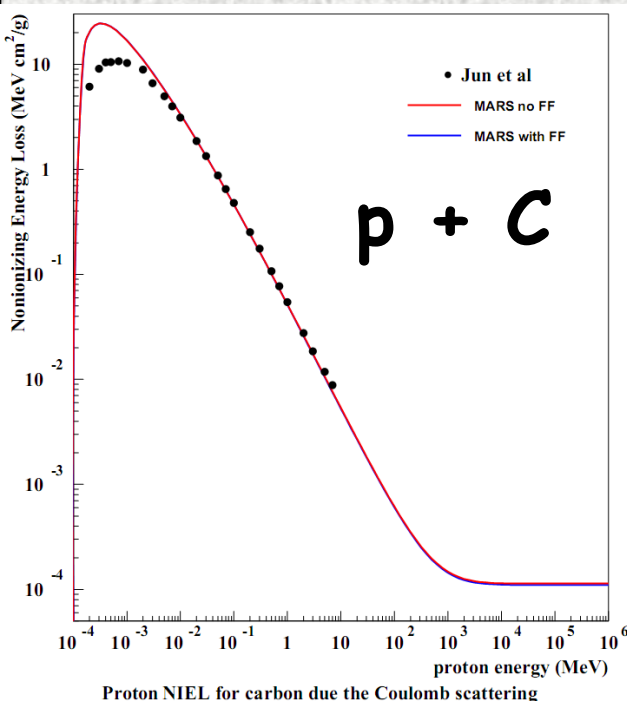


R. Stoller (2000), G. Smirnov

All products of elastic and inelastic nuclear interactions as well as Coulomb elastic scattering of transported charged particles (hadrons, electrons, muons and heavy ions) from 1 keV to 10 TeV. Coulomb scattering: Rutherford cross-section with Mott corrections and **nuclear form factors for projectile and target** (important for high-Z projectiles and targets, see next two slides).

Comparing MARS15 with Most Recent Models

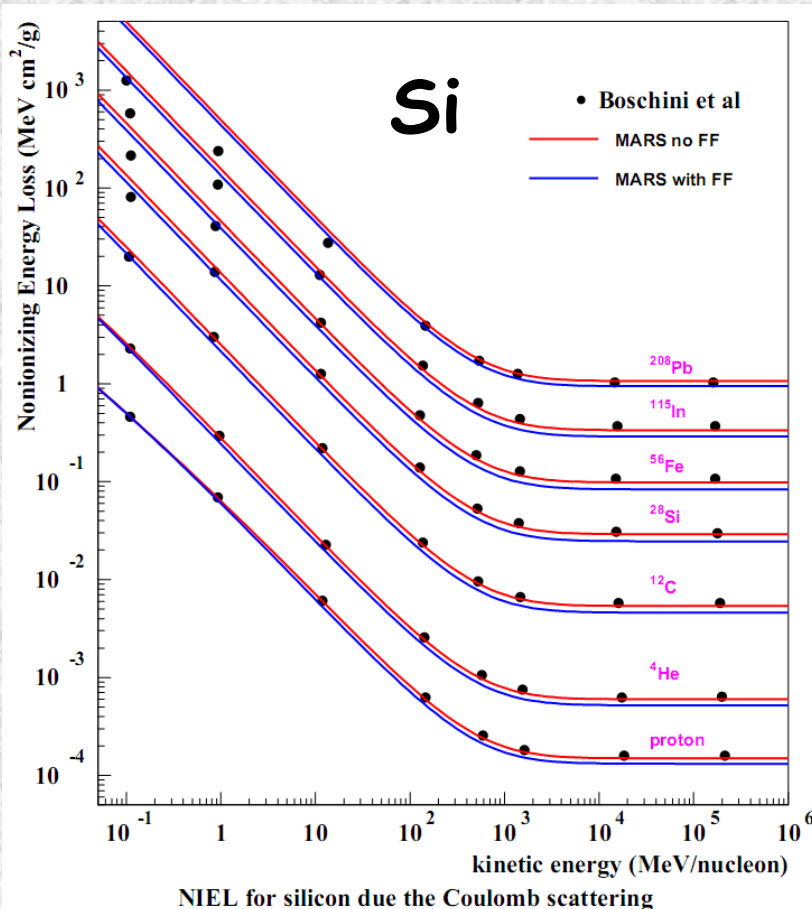
I.Jun, "Electron Nonionizing Energy Loss for Device Applications",
IEEE TRANSACTIONS ON NUCLEAR SCIENCE, VOL. 56, NO. 6, DECEMBER 2009



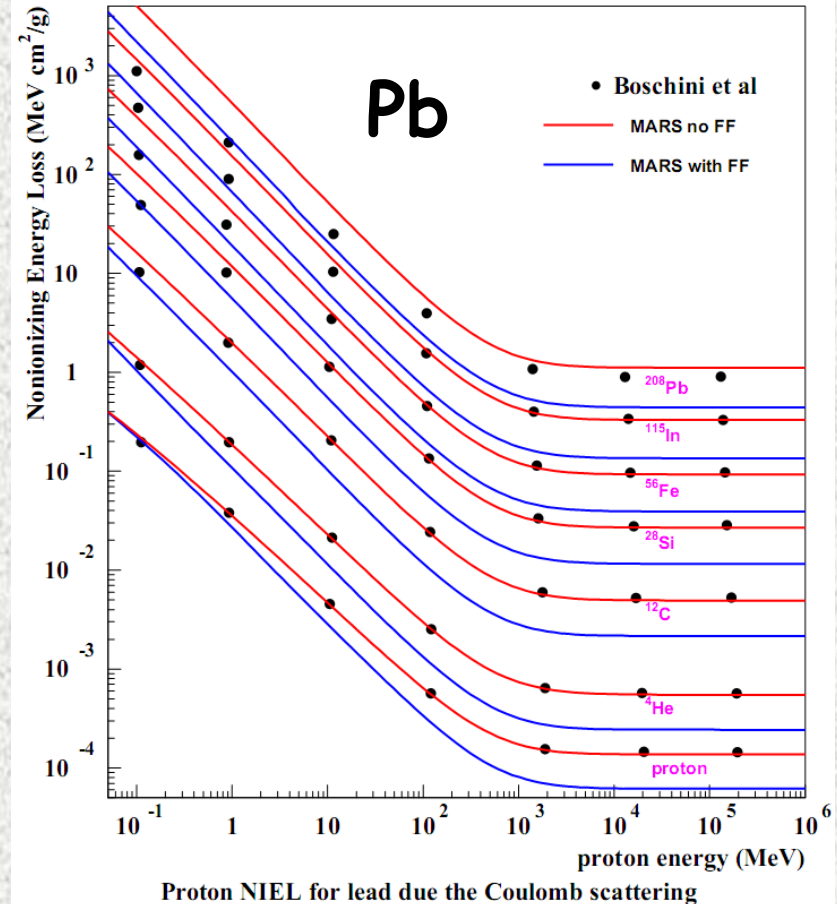
- Minimal proton transport cutoff energy in MARS is 1 keV

Comparing MARS15 with Most Recent Models

M.J. Boschini et al., "Nuclear and Non-Ionizing Energy-Loss for Coulomb Scattered Particles from Low Energy up to Relativistic Regime in Space Radiation Environment", arXiv:1011.4822v6 [physics.space-ph] 10 Jan 2011



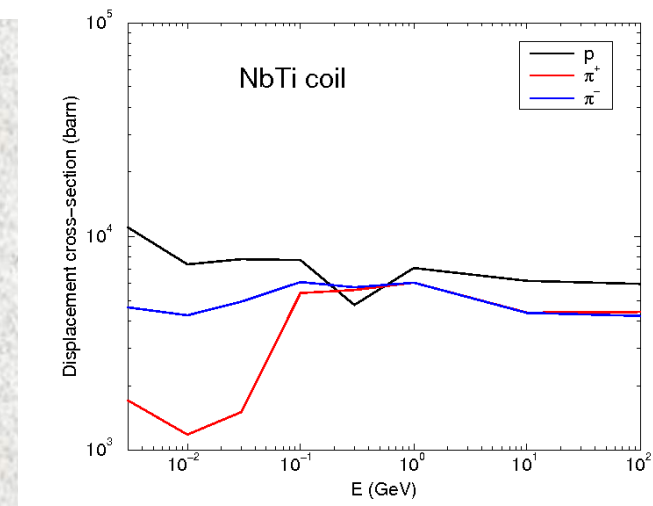
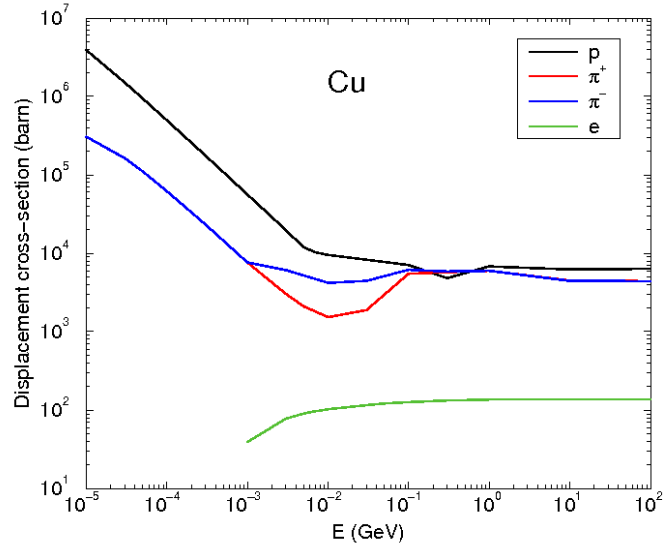
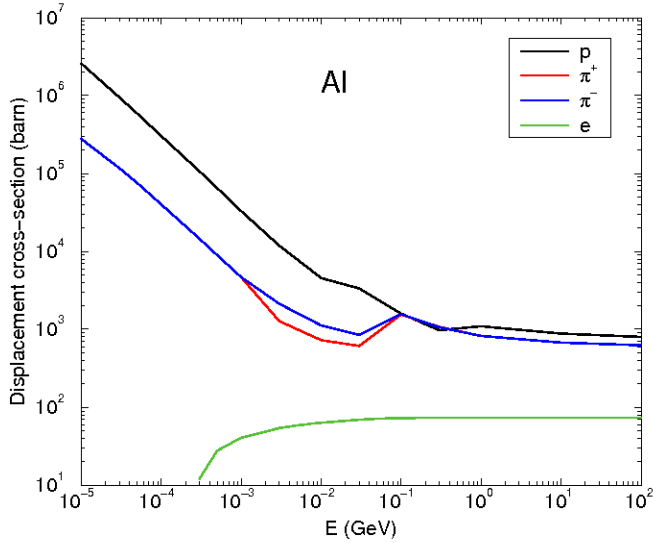
NIEL for silicon due the Coulomb scattering



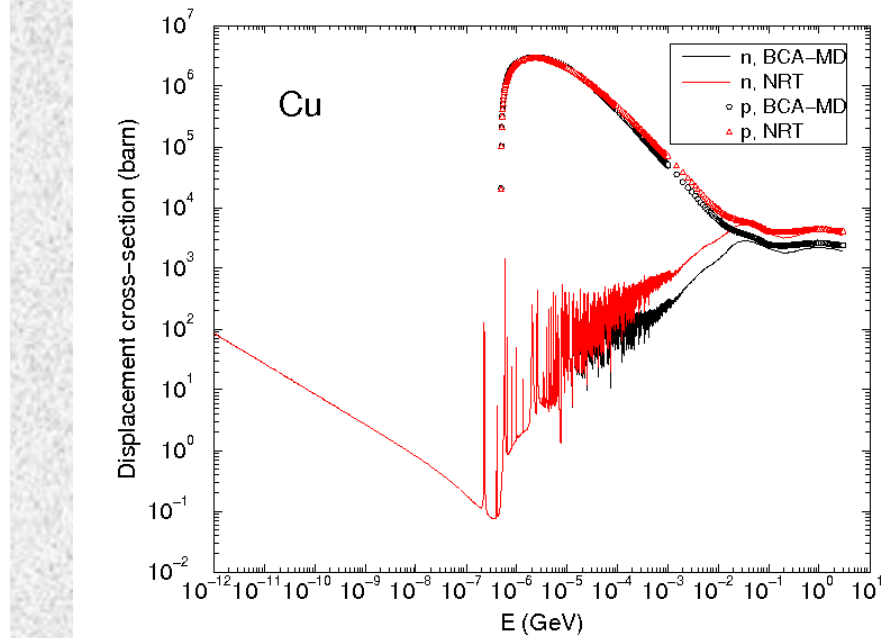
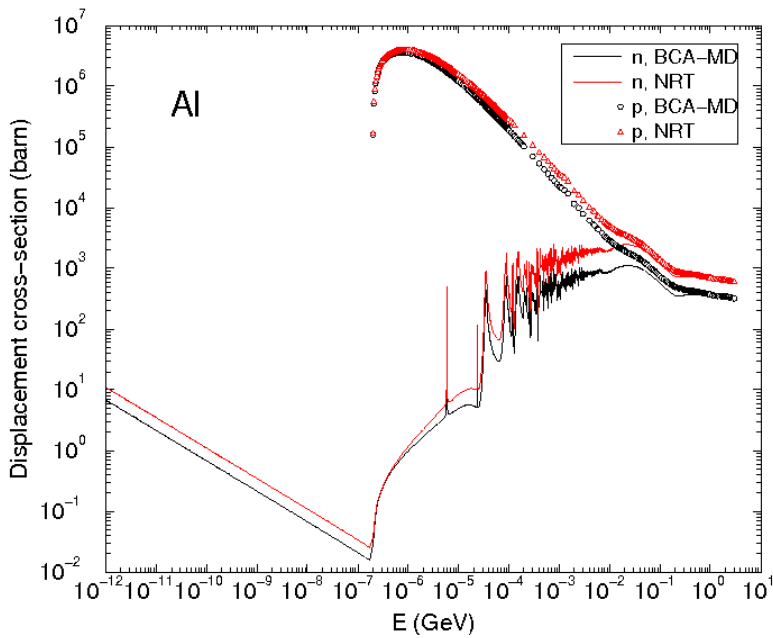
Proton NIEL for lead due the Coulomb scattering

MJB et al. do not include form factors of target and projectile (default in MARS15), which are substantial for high Z

p, π, e Displacement x-sect. in Al, Cu and NbTi Coil

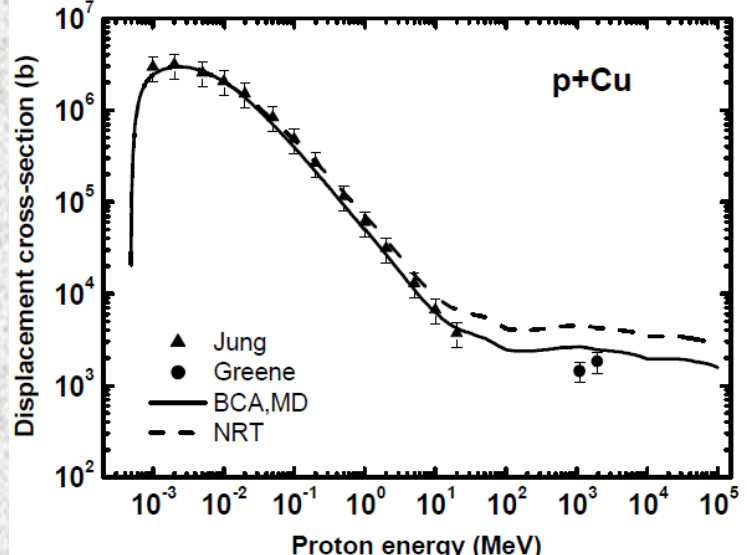
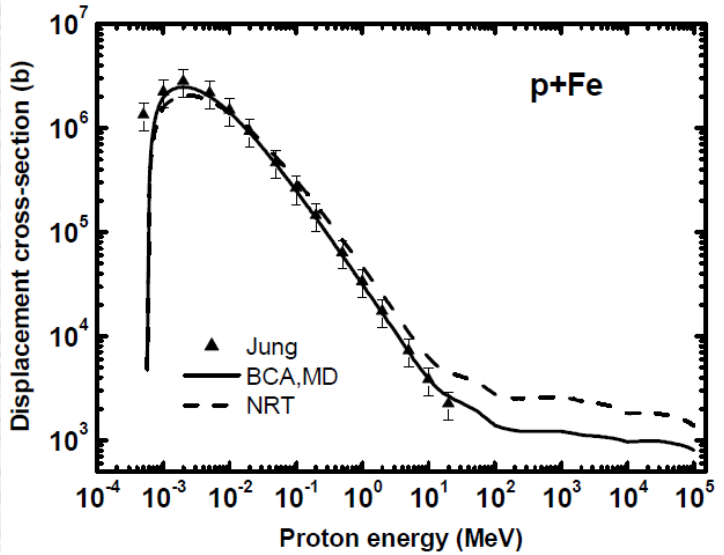


Nucleon Displacement x-section in Al and Cu

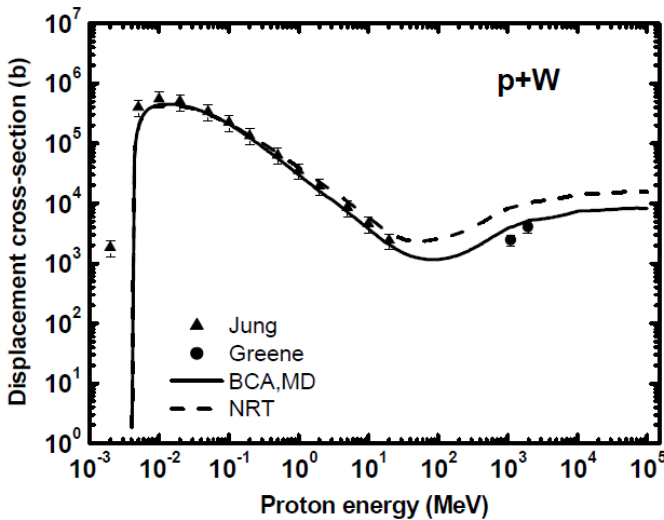


BCA-MD and pure NRT models can differ by a factor of two

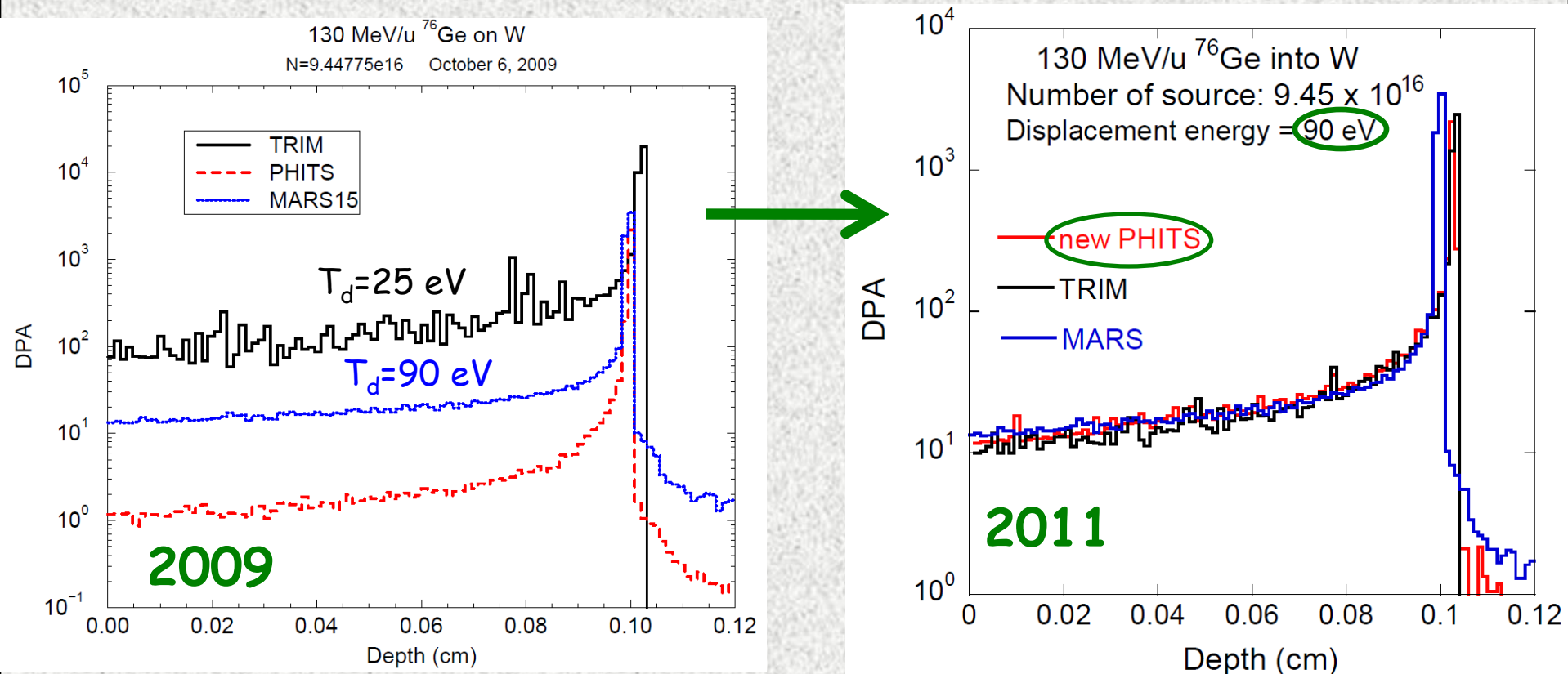
BCA-MD vs NRT vs Data for p+Fe, p+Cu, p+W



Jung data derived from resistivity degradation



DPA Comparison: 130 MeV/u ^{76}Ge on W



Pencil beam, uniform in $R=0.03568 \text{ cm}$ disc.

Target W_{nat} , cylinder with $R=0.03568 \text{ cm}$, $L=0.12 \text{ cm}$

Old PHITS: $T_d=90 \text{ eV}$, no Coulomb elastic

**Include all processes,
use correct parameters**

TRIM and PHITS results: Courtesy Yosuke Iwamoto

DPA Calculation Comparisons (1)

0.32-GeV/u ^{238}U on 1-mm Be, 9 cm² beam

* Courtesy Susana Reyes (2009)

Code	SRIM*	PHITS*	MARS15
DPA/pot	2.97e-20	5.02e-22	2.13e-20

6.50e-20, new PHITS by Yosuke Iwamoto (2011)

Dominant for high-Z projectiles in thin targets

MARS15: Physics process (%)

Nucl. Inel.	EM elastic	L.E. neutron	e^\pm
0.3	99.06	0.02	0.62

DPA Calculation Comparisons (2)

1-GeV p on 3-mm Fe, 1 cm² beam

* Courtesy Susana Reyes (2009)

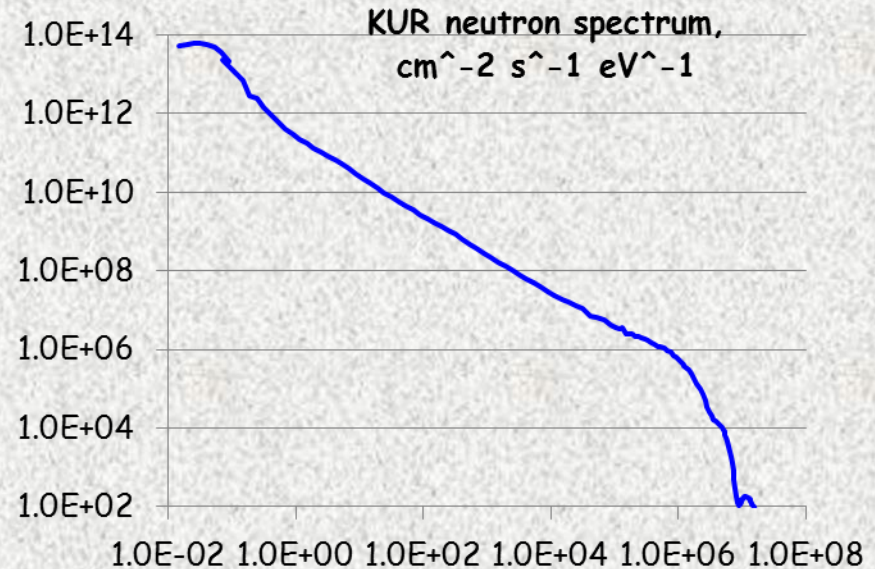
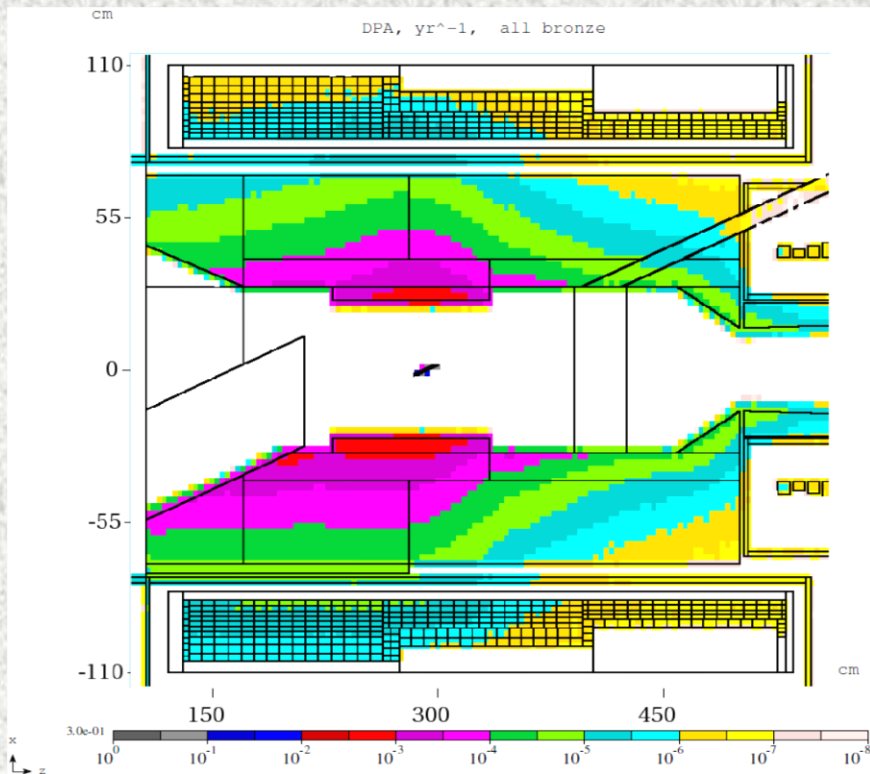
Code	SRIM*	PHITS*	MCNPX*	MARS15
DPA/pot	1.18e-22	2.96e-21	3.35e-21	8.73e-21

7.79e-21, new PHITS by Yosuke Iwamoto (2011)

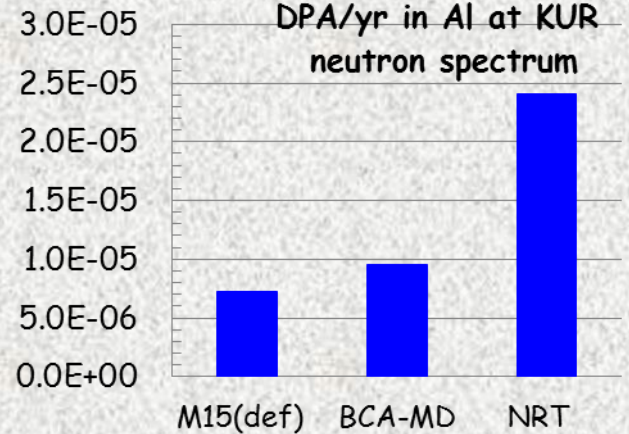
MARS15: Physics process (%)

Nucl. Inel. & Coulomb	Nucl. Elastic	L.E. neutron	e [±]
78.25	16	5.5	0.25

Mu2e Experiment and Neutron Tests at Kyoto Reactor



Derived from resistivity degradation

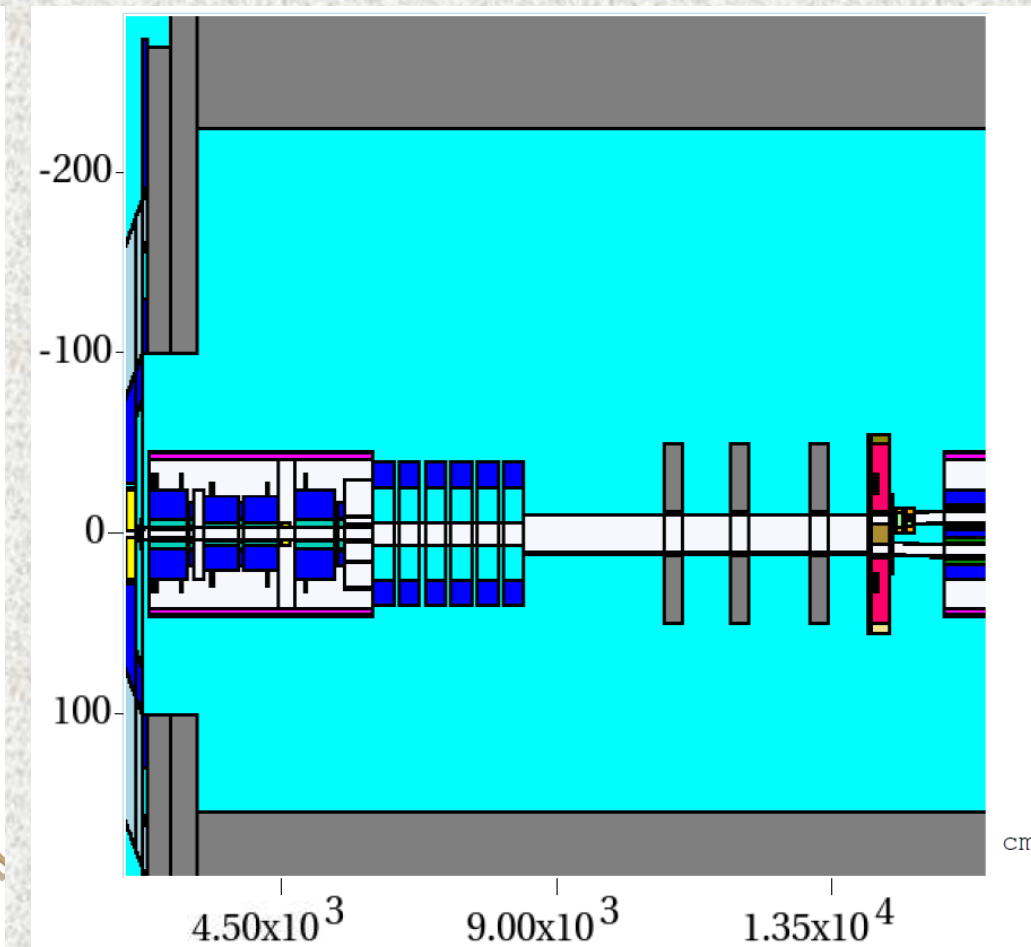
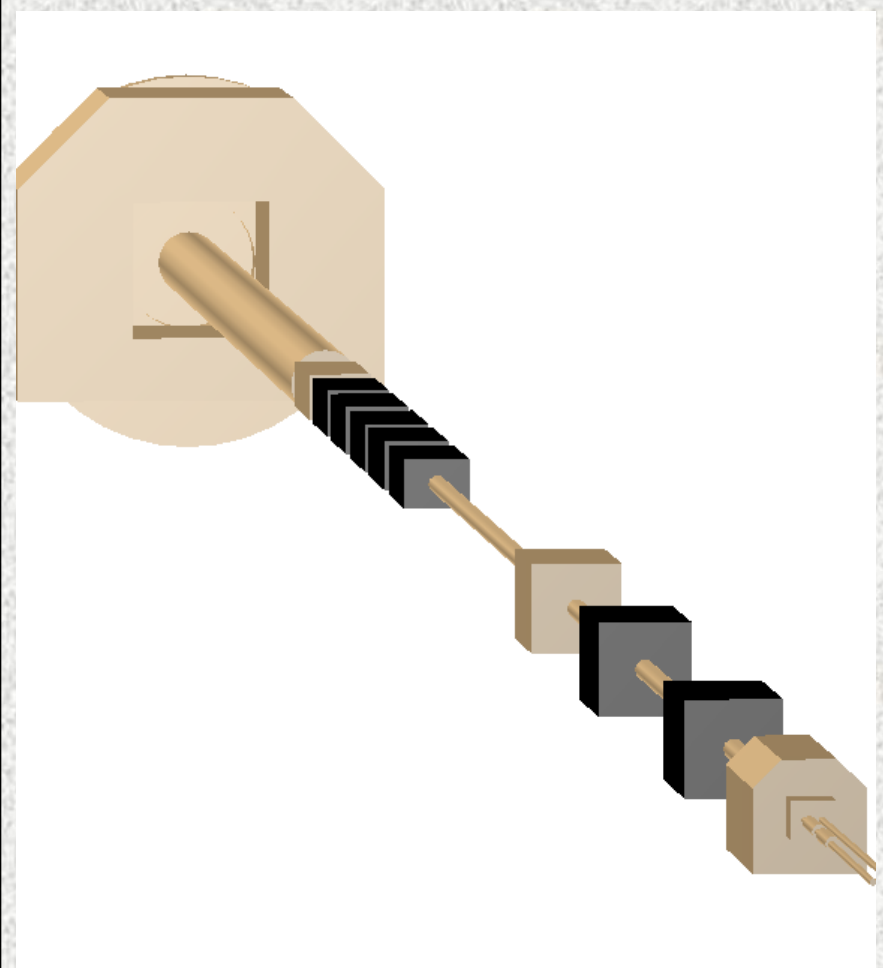


Tests at Reactors and Low Temperatures

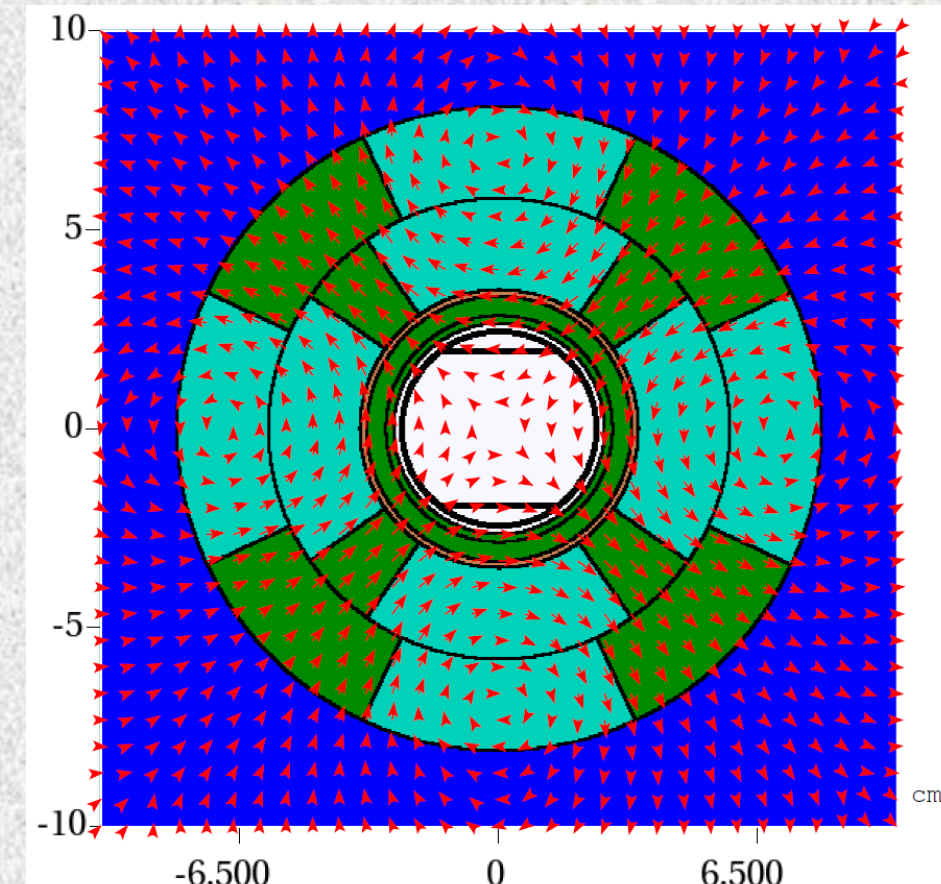
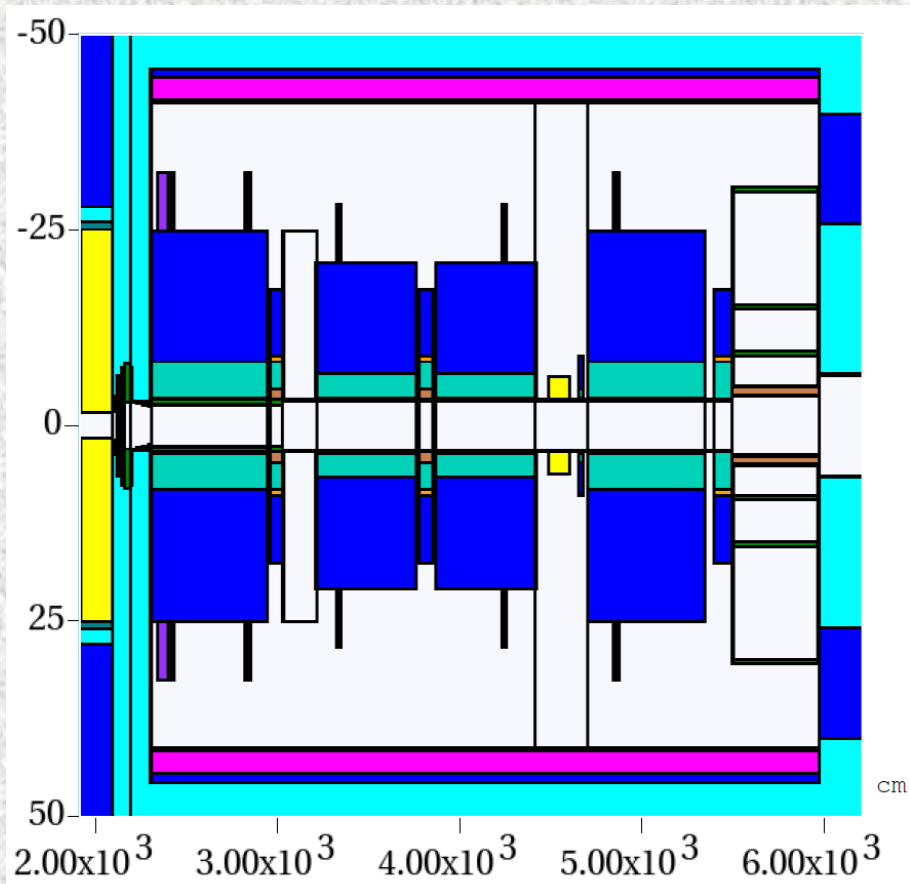
Ratio of number of single interstitial atom vacancy pairs produced in material to number of defects calculated by NRT model

Material	Theo (MD)	Exp
Fe	0.32 ± 0.1	0.32 ± 0.05
Cu	0.27 ± 0.03	0.32 ± 0.03
Ratios exp/MD		
Ti		2
Zr		2
W		2

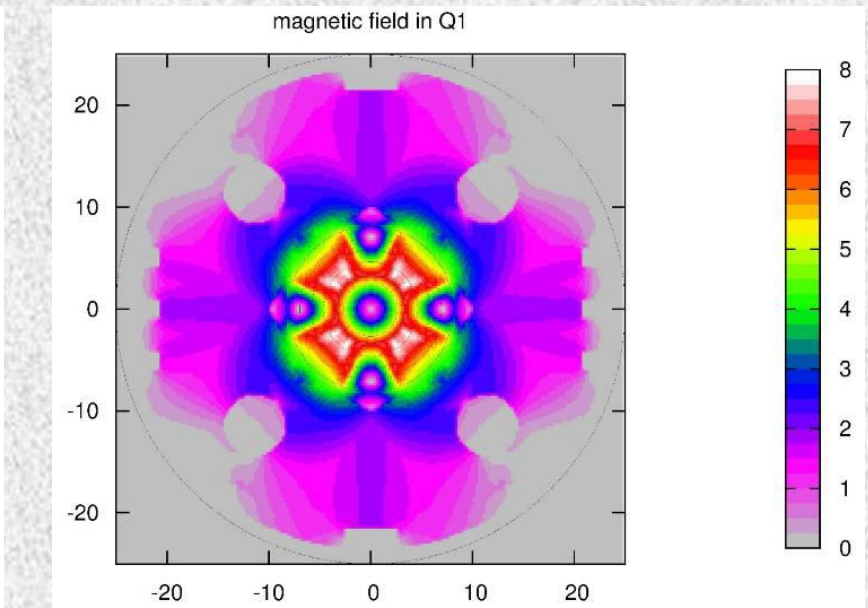
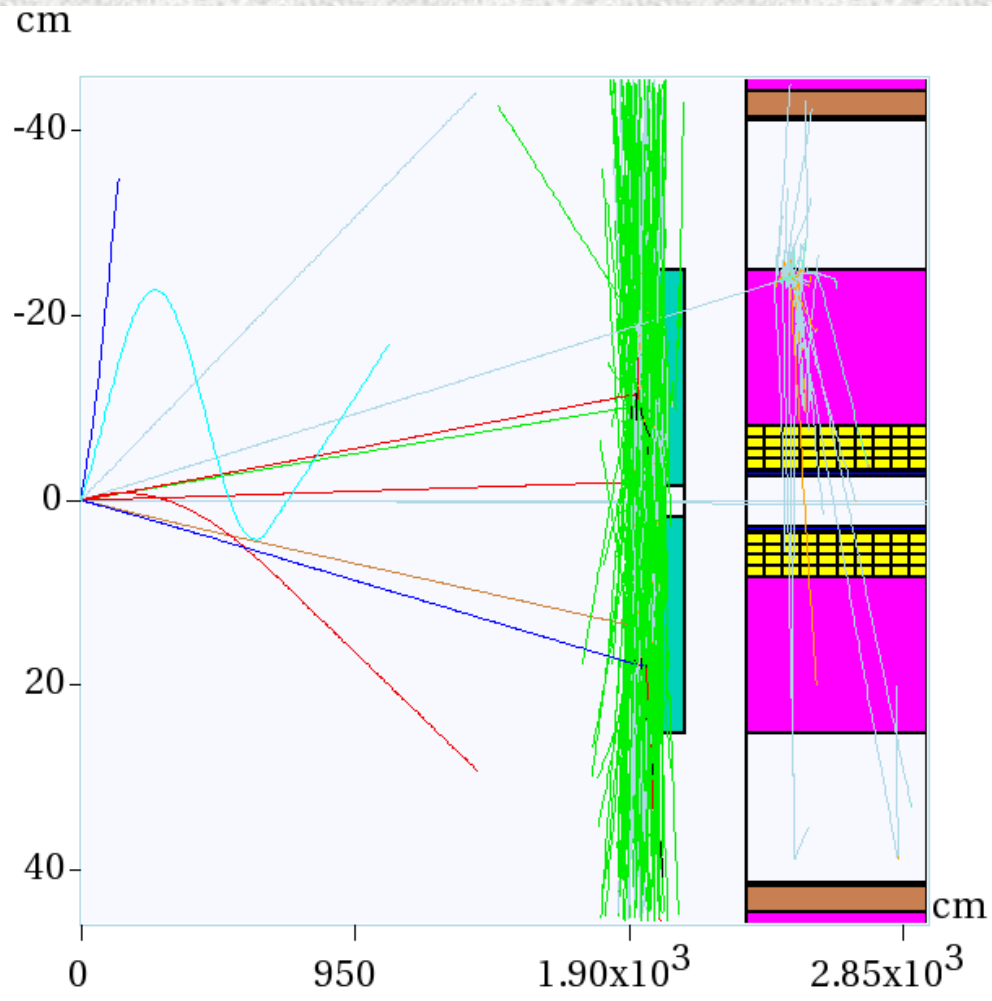
LHC IR5 MARS15 Model



Triplet MARS15 Model



IR5 Inner Triplet Simplified Model



Running FLUKA and MARS
for $\sqrt{S} = 14$ TeV and $L=10^{35}$
(2008)

FLUKA 2006.3 and MARS15 (2007) Intercomparison

Total heat loads in the insertion region elements (W) for upgrade luminosity $L=10^*L_0$

	FLUKA	+/- (%)	MARS	+/- (%)	Ratio FLUKA/MARS
TAS	1853.7	0.5	1827.3	0.7	1.01
Beam pipe	89.1	1.0	97.9	0.4	0.91
Q1 cable	158.0	0.6	159.1	0.2	0.99
yoke	96.3	0.9	78.5	0.4	1.23
aluminium layer	2.3	0.6	2.4	0.5	0.98
mylar insulation	19.5	0.8	20.4	0.3	0.96
stainless steel vessel	16.8	0.8	17.3	0.3	0.97

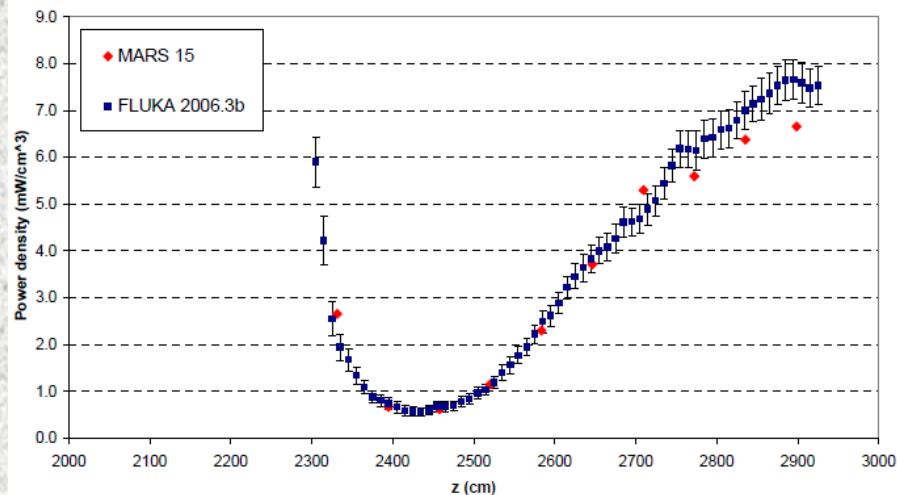


Figure 8: Azimuthal averaged power density in cable1 along Q1

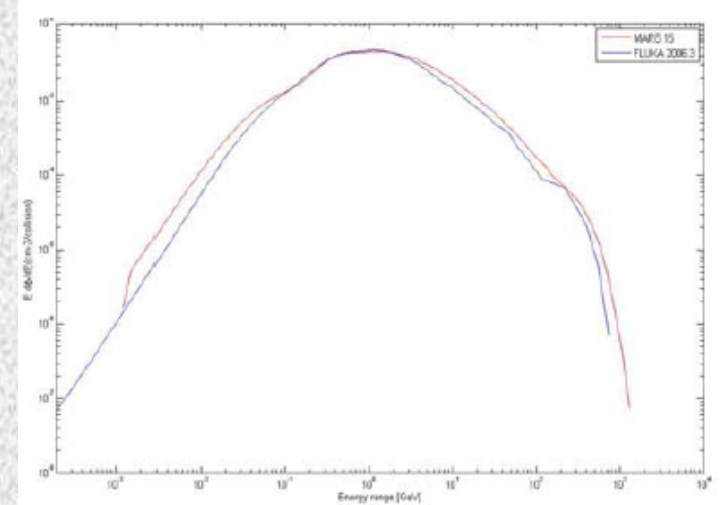
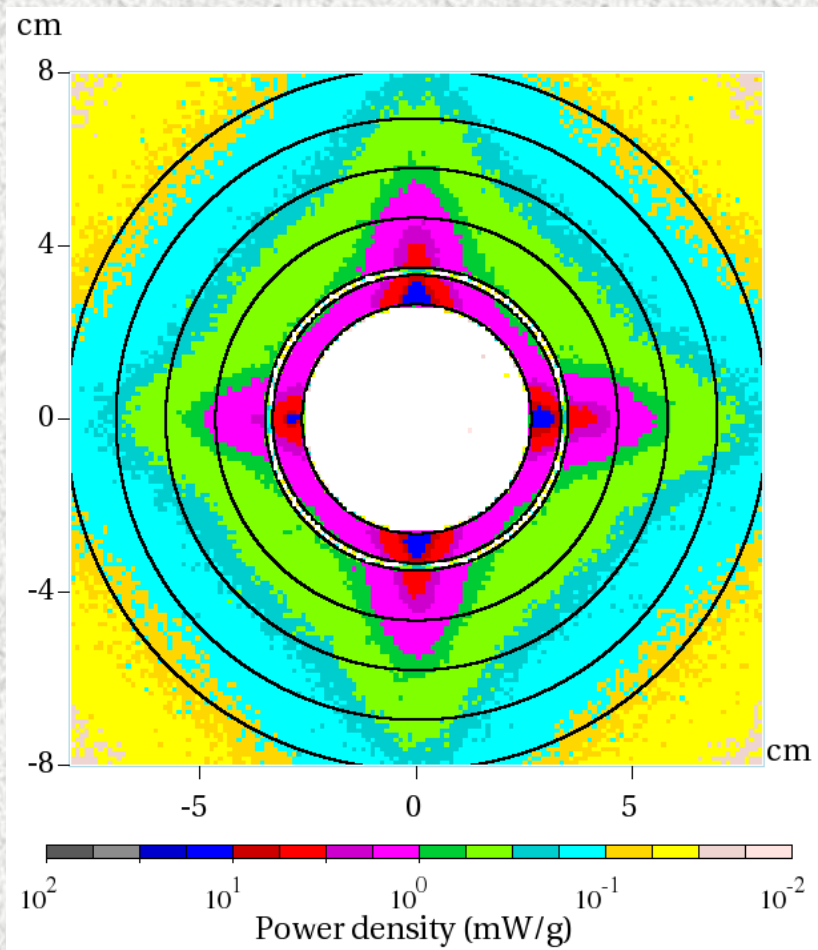
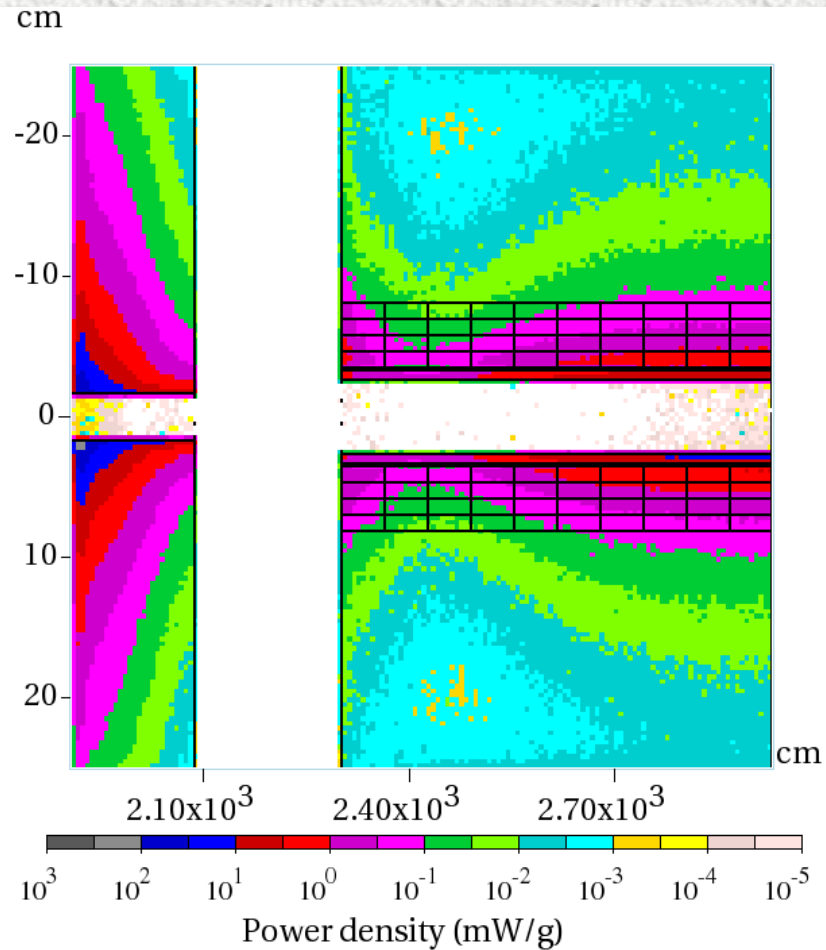


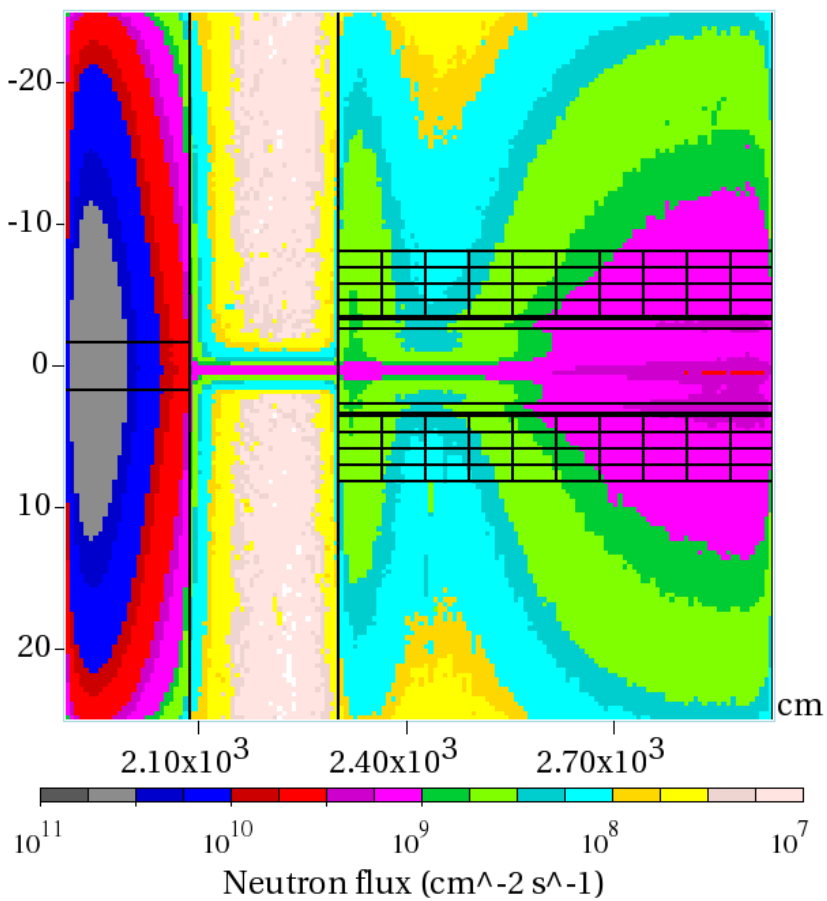
Figure 12: Pion and kaon spectra in cable1

Power Density

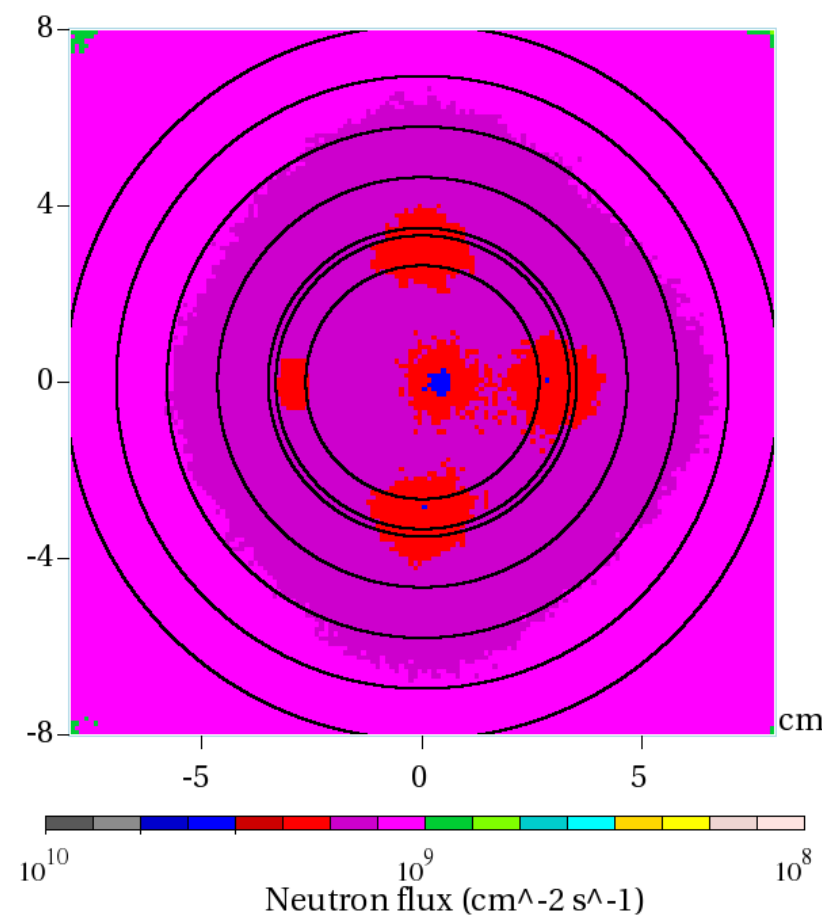


Neutron Flux

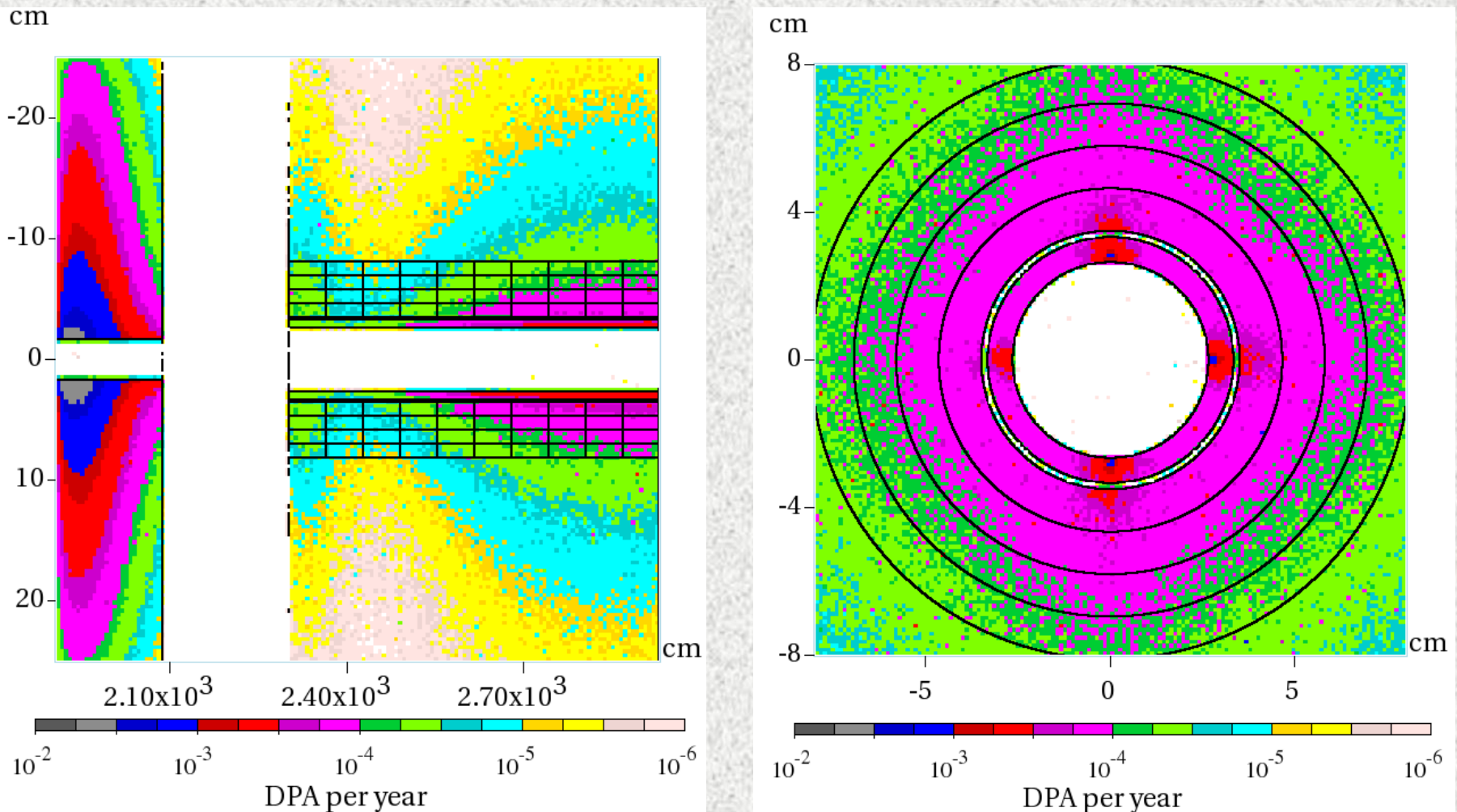
cm



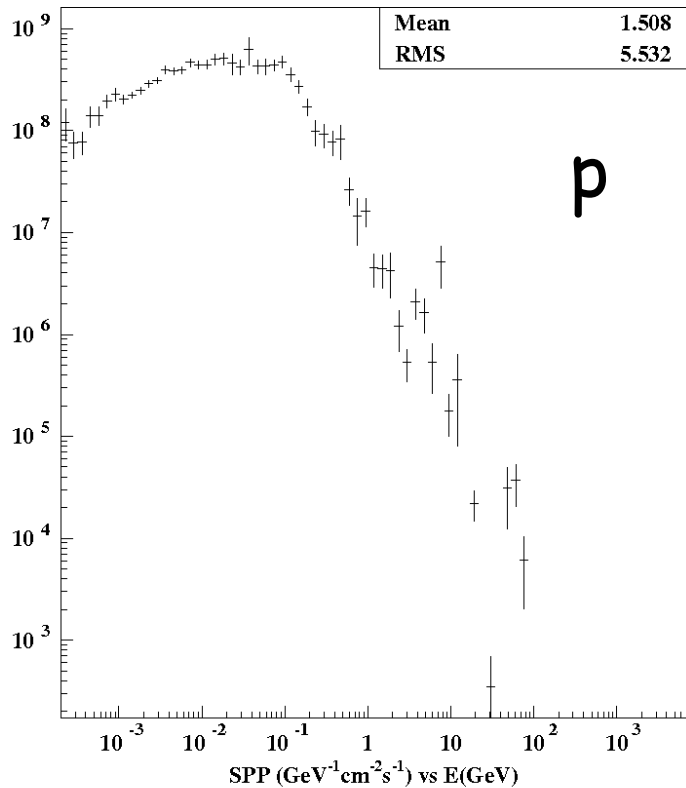
cm



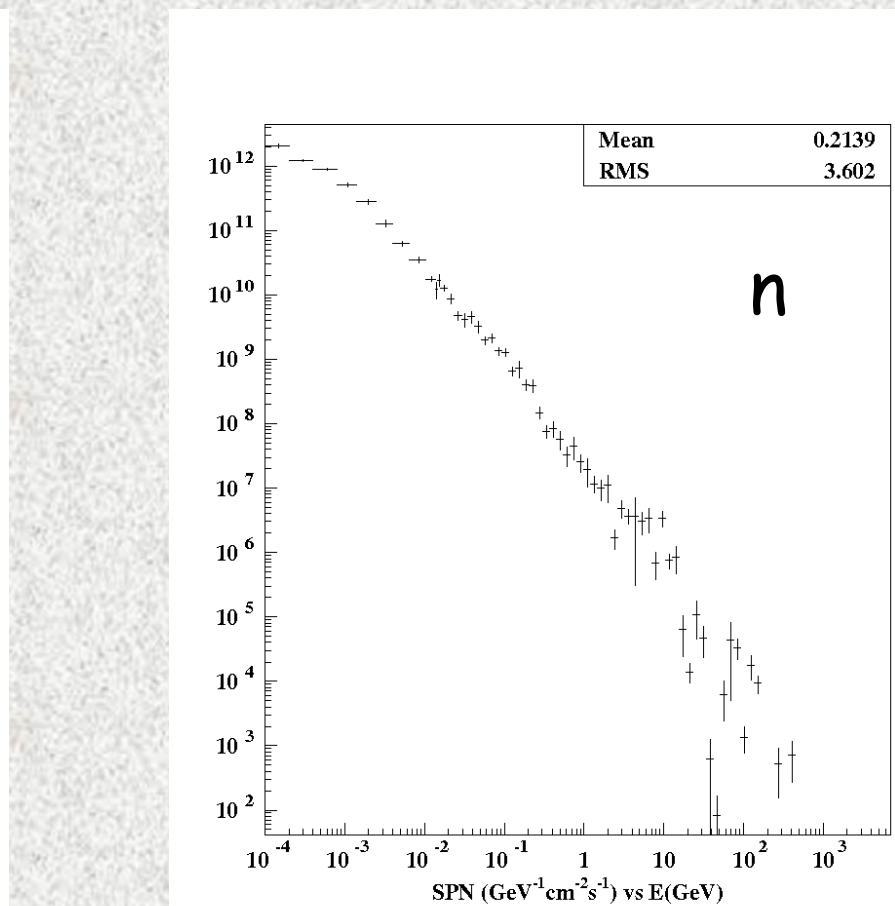
DPA



Nucleon Spectra at Hottest Spot



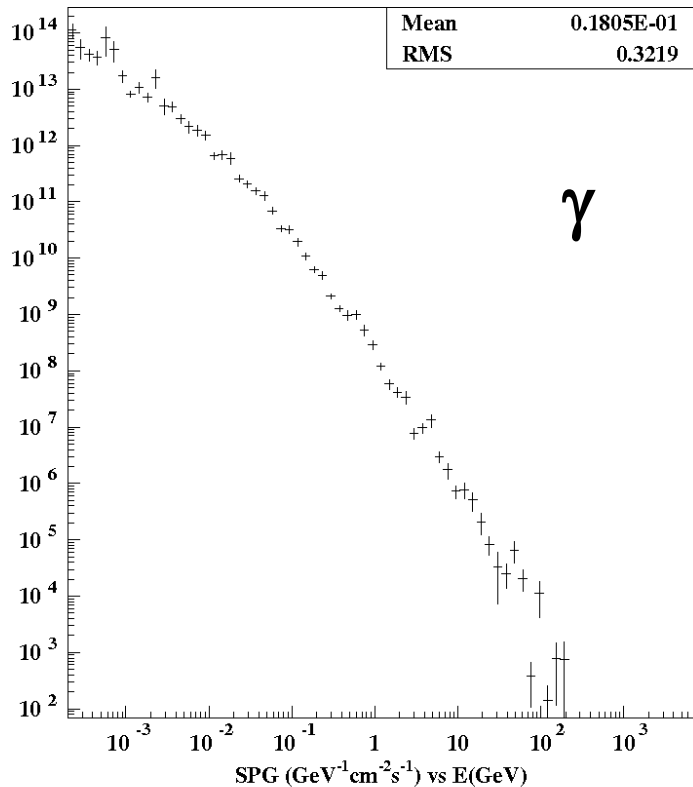
p



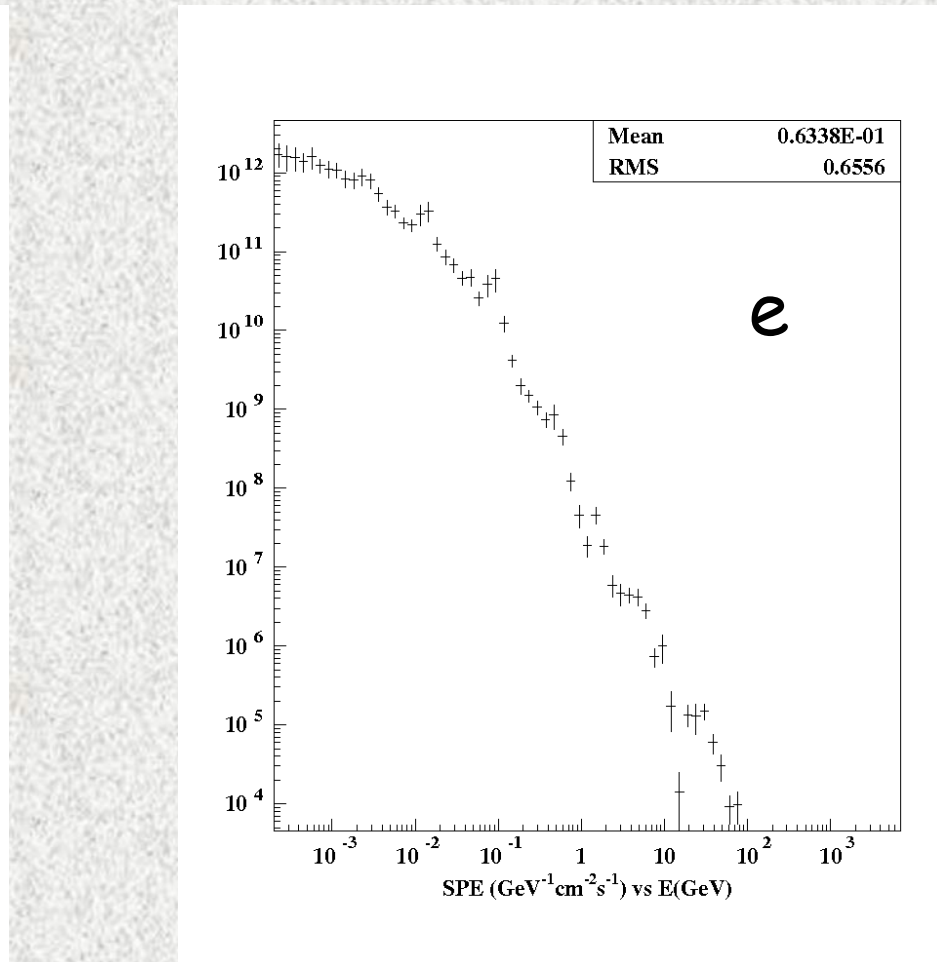
n

1×1×80 cm of inner coil at non-IP end

Photon and Electron Spectra at Hottest Spot



γ



e

1x1x80 cm of inner coil at non-IP end

Mean Energy, Flux and DPA averaged over 4 Hot Spots (L, R, T, B)

Particle j	$\langle E \rangle$ (GeV)	RMS (GeV)	Flux ($\text{cm}^{-2}\text{s}^{-1}$)	DPA/yr	DPA (%)
p	2.93	10.7	$1.3\text{e}8$	$1.75\text{e}-5$	5
n	0.22	3.7	$2.3\text{e}9$	$8.24\text{e}-5$	26
π, K	13.8	41.6	$5.4\text{e}8$	$4.78\text{e}-5$	15
μ	11.3	19.7	$6.3\text{e}5$	$1.70\text{e}-9$	-
γ	0.018	0.35	$8.6\text{e}10$	$\sim 2.\text{e}-5$	6
e	0.077	0.5	$9.8\text{e}9$	$2.47\text{e}-5$	8
Sub-thresh.					40

Sub-thresh = j-particles with $E < 100 \text{ keV}$ + all fragments

Summary (1)

- Modern models/codes which include Coulomb elastic scattering (crucial for high-Z projectiles), nuclear interactions, and same DPA model parameters agree quite well between each other and with (indirect) data. At the same time, industry standard NRT and state-of-the-art BCA-MD differ by a factor of 2 to 3 in some cases.
- Strong dependencies on projectile type and energy (1 keV to a few GeV), projectile/target charge and nuclear form-factor and material properties are shown and can be further studied with modern models/codes.

Summary (2)

- Independent FLUKA and MARS results on energy deposition (mostly from EMS) for inner triplet coils are in agreement within a few %, therefore one can predict dose in insulator with same accuracy.
- Uncertainties on DPA predictions in superconductors can be as high as a factor of 2 to 3.
- MARS15 results are obtained on composition of particle flux and DPA in the hottest spots of the final focus quadrupole superconducting coils.
- The major contributors to DPA are sub-threshold particles (40%), neutrons > 100 keV (26%) and pions (15%).